INTERNATIONAL JOURNAL OF PRECISION ENGINEERING AND MANUFACTURING Vol. 14, No. 6, pp. 919-924 JUNE 2013 / 919
DOI: 10.1007/s12541-013-0121-z

A Nonlinear Control of an QZS Isolator with Flexures Based on a Lyapunov Function

Pham Van Trung[1], Kyoung-Rock Kim[1], and Hyeong-Joon Ahn[2,#]

1 Graduate School, Department of Mechanical Engineering, Soongsil University, 511 Sangdo-dong, Dongjak-gu, Seoul, South Korea, 156-743
2 Department of Mechanical Engineering, Soongsil University, 511 Sangdo-dong, Dongjak-gu, Seoul, South Korea, 156-743
Corresponding Author / E-mail: ahj123@ssu.ac.kr, TEL: +82-2-820-0654, FAX: +82-2-820-0668

KEYWORDS: Active QZS vertical isolator, Horizontal indirect actuation, Nonlinear control, Lyapunov function

This paper presents an active control method for a quasi-zero stiffness (QZS) isolator using flexures based on a Lyapunov function. First, shown is a dynamic model of an active QZS isolator having indirect horizontal actuation. In the model, the control force is applied along the horizontal direction to compensate for vertical vibrations. Next, a nonlinear control algorithm for the active isolator is developed based on a Lyapunov function. Simulation of the active isolator model which consists of passive QZS isolators, sensors and actuator dynamic models is done to study the effects of control tuning gain on the system performances. In order to verify the active isolation performances, developed is an experimental model including an active QZS isolator, an exciter device and various sensors. Finally, experiments for such as impulse disturbance rejection and transmissibility are performed and the results show that the indirect horizontal actuation by the active QZS isolator using flexure attenuates impulse disturbance as well as isolates the base vibration effectively.

Manuscript received: October 24, 2012 / Accepted: April 3, 2013

NOMENCLATURE

$A_{1\text{-}3}$	Coefficients of nonlinear model of notched flexure
$a_{1\text{-}3}$	Control gains
$B_{1\text{-}3}$	Coefficients of Lyapunov functions
C,c	Dimensional and non-dimensional damping coefficient of the isolator system
f	Non-dimensional vertical restoring force of the flexures
F_{ch}, f_{ch}	Dimensional and non-dimensional control force produced by the horizontal actuator
f_{cv}	Non-dimensional control force produced by the horizontal actuator
f_{mg}	Non-dimensional weight of the payload
G_s	The transfer function of a sensor
k_h, k_v	Non-dimensional stiffness of horizontal and vertical spring
K_l, k_l	Dimensional and non-dimensional linear stiffness of the isolator
K_n, k_n	Dimensional and non-dimensional nonlinear stiffness of the isolator
$L, \dot{L}$	The Lyapunov function and its derivative
L_a, L_b	Length of the notched and thick parts of the flexure
M, m	Dimensional and non-dimensional supported mass
M_B	Base mass
n	Flexure shape ratio (L_b/L_a)
g	Number of flexures
p	Non-dimensional compression force
p_0	Non-dimensional initial compression force
s	The number of flexures in one lateral side of the isolator.
T_1, T_2	Coefficients for flexure stiffness
x_l	Non-dimensional horizontal parasitic motion of flexure at right end of flexure
y	Non-dimensional vertical coordinate
y_0	Non-dimensional initial deflection of vertical spring for gravity compensation
Y_B	Base excitation
Y_m, y_m	Dimensional and non-dimensional vertical displacement of payload mass
z_1, z_2	System states for Lyapunov function
$W(t), w(t)$	Dimensional and non-dimensional external disturbance force
ω_c	Cut-off frequency of the sensor
ξ	Damping ratio of the sensor model

1. Introduction

Recently, a growing interest in the study of nonlinear isolation has arisen to overcome the inherent drawback of the linear isolator.[1] In the linear isolator, a smaller stiffness resulting in a wider frequency range of isolation causes the problem of undesired static deflection.[2,3] A desirable vibration isolator should possess high-static–low-dynamic stiffness so that it can support a large load statically while having low dynamic stiffness to enlarge frequency ranges of vibration isolation. When an isolator has zero or near zero dynamic stiffness, it is referred to as a quasi-zero-stiffness (QZS) isolator.

Although various configurations of passive QZS isolators have been proposed and studied,[1,6-12] the passive isolators still have a couple of dynamic limitations.[11] For example, passive QZS isolators respond very weakly to impulsive force since they have almost zero dynamic stiffness near the operating point. In addition, the nonlinear dynamic characteristic of the QZS isolators may cause chaotic vibration responses at resonance frequencies.[11] Accordingly, the active QZS isolators were studied and investigated to improve and optimize the isolation performance. Recently, some studies were made available on the active QZS isolators using simulation,[13] but few experimental researches have been done on the active QZS isolators.[14,15]

In this paper, presented is an active nonlinear control method using a quasi-zero stiffness isolator based on a Lyapunov function. In this method, a vertical QZS isolator using flexures is controlled indirectly by horizontal actuation using a voice coil actuator. A nonlinear control force for active isolation is derived from the Lyapunov function and then the effects of nonlinear control gains are studied through simulations. Finally, a testing model is built to investigate system responses to impulse disturbance and transmissibility. In both simulation and experiment, it is shown that good disturbance rejection characteristics and vibration isolation performances are obtained using the active QZS isolator with indirect horizontal nonlinear actuation.

2. Active Control for QZS Isolator with Flexure

2.1 The QZS isolator using flexure

The QZS isolator using flexures is shown in the Fig. 1(a). Also, shown in the Fig. 1(b) is the schematic diagram of the passive isolator. The QZS isolator consists of flexures, vertical spring, horizontal spring and vertical gravity compensator, as shown in Fig. 1(a). Although the flexure has positive stiffness without any compression force, stiffness of the flexure becomes negative as the compression force is increased by preloading of horizontal spring at the right end of flexure. Finally, the isolator has nearly zero stiffness as the compression force increases, which means low dynamic stiffness. In addition, a gravitation compensation device is installed under the vertical coil spring. The worm gear lifts the spring support upward (y_0) and increases preload of the vertical spring to compensate the initial sag of the payload, which means high static stiffness.

2.2 Dynamic model of the QZS isolator using flexures[16,17]

Applying the second Newton's law to the model in the Fig. 1(b), the motion equation of the payload mass on the QZS isolator's top is expressed as

$$m\ddot{y}_m = -f_{mg} - c\dot{y}_m - k_v(y_m + y_0) + f + w(t) \tag{1}$$

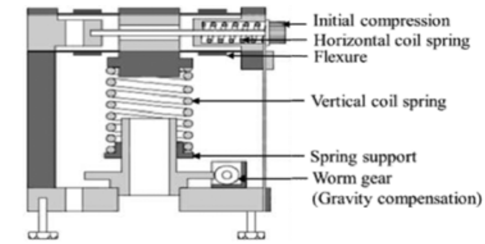

(a) Mechanism[5]

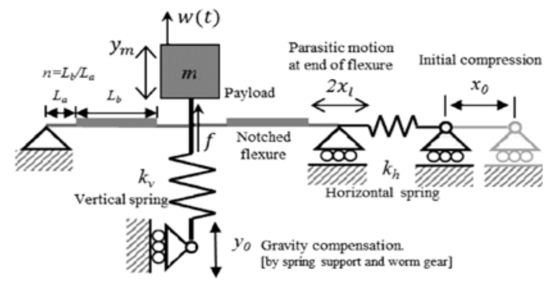

(b) Schematic diagram

Fig. 1 The vertical QZS isolator using flexures

Here, all variables are non-dimensional.

The vertical restoring force (f) of the flexure is obtained through the following steps. The first step of conversion from bidirectional vertical motion (y_m) of the payload mass to a small horizontal parasitic unidirectional motion (x_l) of the flexure can be expressed approximately as Eq. (2).

$$x_l = A_3 y_m^2 \tag{2}$$

Secondly, the horizontal parasitic motion (x_l) of flexures perturbs initial deflection of horizontal spring or compression force (p_0 - $2k_h x_l$) on flexures. Since the total compression force is shared by s flexures at one side, a compression force applied to each side can be shown as Eq. (3),

$$p = (p_0 - 2k_h x_1)/s \tag{3}$$

Finally, a total vertical restoring force (f) produced by the flexures is obtained by summation of all the vertically paralleled restoring forces of every flexure in both sides of the mode, as shown in Eq. (4),

$$f = g y_m (A_1 - A_2 P) \tag{4}$$

where, $A_1 = \dfrac{6}{3n^2 + 6n + 4}$, $A_1 = \dfrac{3n+2}{3n^2+6n+4} + \dfrac{8}{5(3n^2+6n+4)^2}$,

$A_3 = \dfrac{3n+2}{2(3n^2+6n+4)} + \dfrac{4}{5(3n^2+6n+4)^2}$, $n = L_a/L_b$, $g = 8$ and $s = 4$.

Assuming that payload weight is compensated by initial deflection of vertical spring (y_0) and substituting Eqs. (2) and (3) into Eq. (4) and the resulting equation into Eq. (1), the final motion equation of the passive QZS isolator using flexures is obtained as shown in Eq. (5). The cubic stiffness denotes small stiffness near the equilibrium point and high stiffness out of the equilibrium point.

$$m\ddot{y}_m + c\dot{y}_m + (k_v + T_1)y_m + T_1 y_m^3 = w(t) \tag{5}$$

where, $T_1 = gA_1 - \dfrac{gA_1 p_0}{s}$ and $T_2 = \dfrac{2gA_2A_3k_h}{s}$.

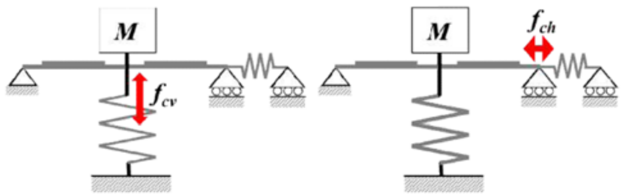

(a) Vertical actuation (b) Horizontal actuation

Fig. 2 Isolator control configurations

2.3 Active control configurations

Two possible control configurations for the QZS isolator using flexures are shown in Fig. 2. Horizontal actuation needs small stroke and large force, while vertical actuation requires large stoke and small force.[18] In case of active isolation, direct vertical actuation is conventionally used as shown in the Fig. 2(a). However, the space for the vertical actuator is limited by the presence of the vertical spring and gravity compensation mechanism under the payload. Therefore, the horizontal actuation is used for active control of the QZS isolator. The isolator's stroke is not limited by the actuator's stroke and the control force can accurately be adjusted because of wide range of required force.

Substituting p_0+f_{ch} into p_0, the equation of the active dynamic model with indirect horizontal actuation force (f_{ch}) is expressed as Eq. (6).

$$m\ddot{y}_m+c\dot{y}_m+k_ly_m+k_ny_m^3=\frac{gA_2y_m}{s}f_{ch}+w(t) \tag{6}$$

where $k_l=k_{vs}+T_1$ is linear stiffness and $k_n=T_2$ is nonlinear stiffness.

The non-dimensional system equation or Eq. (6) can be dimensionalized as Eq. (7) by multiplying El/L_a^2 and substituting Y_m/L_a into y_m.

$$M\ddot{Y}_m+C\ddot{Y}_m+K_lY_m+K_lY_m^{\ 3}=\frac{gA_2y_m}{sL_a}F_{ch}+W(t) \tag{7}$$

In case of base excitation, dynamic equation can be easily obtained by replacing Y_m as (Y_m-Y_B) and $W(t)$ as $M_B\ddot{Y}_B$, respectively.[19]

3. Nonlinear Control based on Lyapunov Function

A nonlinear feedback control against impulse force to payload is focused in this paper. In particular, a nonlinear control rule for Eq. (6) is derived using Lyapunov's stability criteria. Letting $z_1=Y_m$, $z_2=\dot{Y}_m$ and substituting these into Eq. (6), we obtain

$$\dot{z}_2=\left(-Cz_2-K_lz_1-K_nz_1^3+\frac{gA_2z_1}{sL_a}F_{ch}+W(t)\right)/M \tag{8}$$

By choosing a Lyapunov function L as Eq. (9), and differentiating the function with respect to time, its derivative yields Eq. (10).

$$L=\frac{1}{2}(B_1z_1^2+B_2z_2^2) \tag{9}$$

$$\dot{L}=B_1z_1\dot{z}_1+B_2z_2\dot{z}_2 \tag{10}$$

In general, the system is asymptotically stable if the following conditions are met: $L\geq 0$ and $\dot{L}\leq 0$. The first condition ($L\geq 0$) is fulfilled by choosing Lyapunov coefficients $B_1,B_2\geq 0$. The second condition ($\dot{L}\leq 0$) is satisfied under assumption of $B_3\geq 0$ and Eq. (11) since $\dot{L}=-\frac{B_1}{B_2}z_1\leq B_3z_2$.

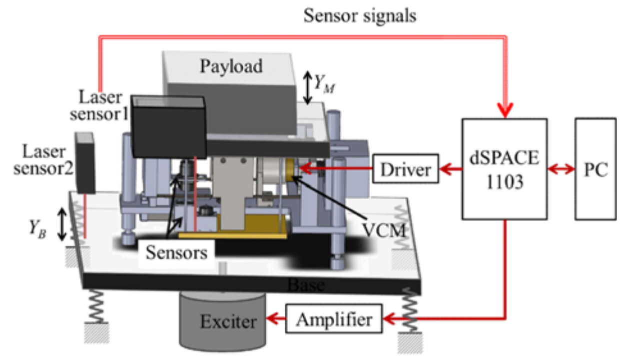

Fig. 3 Experimental setup

$$\dot{z}_2=-\frac{B_1}{B_2}z_1-B_3z_2 \tag{11}$$

The nonlinear control rule can be determined as Eq. (12) by substituting Eq. (8) into Eq. (10).

$$F_{ch}=\left(K_l-\frac{B_1}{B_2}M\right)\frac{sLa}{gA_2}\frac{z_1}{z_1}+(c-B_3M)\frac{sLa}{gA_2}\frac{z_2}{z_1}-K_n\frac{sLa}{gA_2}\frac{z_1^3}{z_1}-\frac{sLa}{gA_2}\frac{W(t)}{z_1} \tag{12}$$

If augmented control gains are introduced and z_1 and z_2 terms are replaced by y_m and $\dot{y}_m$, respectively, Eq. (12) can be simplified as Eq. (13).

$$F_{ch}=a_1\frac{y_m}{\max(y_m,y_0)}+a_2\frac{\dot{y}_m}{\max(y_m,y_0)}+a_3\frac{y_m^3}{\max(y_m,y_0)} \tag{13}$$

where a_1, and a_2 are displacement and velocity gain, respectively, a_3 is nonlinear gain to cancel the system nonlinear characteristic. The values of a_1, a_2, and a_3 are chosen in consideration of Eq. (13) for system stability. The $\max(y_m, y_0)$ is introduced to prevent the actuator saturation and chattering while the supported mass operates at the equivalent position $Y_m=0$.

4. Experiment Configuration Setup

The experimental set-up consists of the passive QZS isolator using flexures, a digital controller, sensors, an actuator and an exciter base, as shown in Fig. 3. The specification of the vertical passive isolator is summarized in Table 1. A voice coil motor (VCM60-25) is used to generate the horizontal control force. Specifications of VCM and its driver are shown in Table 2. A DSP control system or DS1103[18] is used to implement the nonlinear control. Several sensors are used: laser displacement sensors (Keyence LK-G80), a gap sensor (XS4-P30AB120), a velocity sensor (Geophones GS-11D) and an accelerometer (TA-25J-02-1). The laser sensors are used for verification of isolation performance while others are used for feedback control. Specifications of the sensors are given in Table 3. The exciter base is comprised of an exciter (HEV 200, Max. force 200N, Stroke 10 mm), a linear amplifier (20 A and 10 V), and an Al top plate and spring.

Table 1 Isolator specifications

Parameter	Value	Parameter	Value
Allowable mass	25 - 48(Kg)	Stroke	± 0.005(m)
Horizontal spring	3.626×10^5(N/m)	Vertical spring	1.02×10^4 (N/m)
Damping	2.87 (Ns/m)	Natural frequency	0.5-1 (Hz)

Table 2 Specifications of VCM and its driver

Max. force	EMF constant	Bandwidth	Resistance	Inductance
119 (N)	7.25 (N/A)	500 (Hz)	5.2 (ohm)	6.42 (μH)

Table 3 Specifications of sensors

Sensors	Range	Bandwidth	Gain	Noise
Laser sensor	±15 (mm)	10 (kHz)	1.5 (mm/v)	$\pm 10^{-5}$ (m)
Gap sensor	1 ~ 15 (mm)	300 (Hz)	1.67 (mm/v)	$\pm 0.5 \times 10^{-4}$ (m)
Velocity sensor	±12 (m/s)	3.5 (Hz)	0.32 (Vs/cm)	0.05 (m/s)
Accelerometer	±18 (m/s^2)	450 (Hz)	0.51 (Vs^2/m)	±0.01 (m/s^2)

Fig. 4 Impulse disturbance rejection

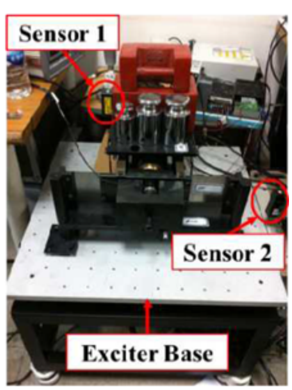

Fig. 5 Transmissibility

Two active isolation performances, namely impulse disturbance rejection and vibration transmissibility, are evaluated experimentally. The experimental set-up for impulse disturbance rejection is shown in Fig. 4. A ball is dropped from a certain height to the top of the isolator. A collision between the ball and the isolator top transmits impulse force to the isolator. Although the controller is designed for disturbance to the payload, stiffness and damping of the closed loop system can be adjusted by the nonlinear control gain and the transmissibility can be improved. Therefore, the isolation performance to the base motion is evaluated by measuring the transmissibility of the closed system. Figure 5 shows the test device to measure the vibration transmissibility,

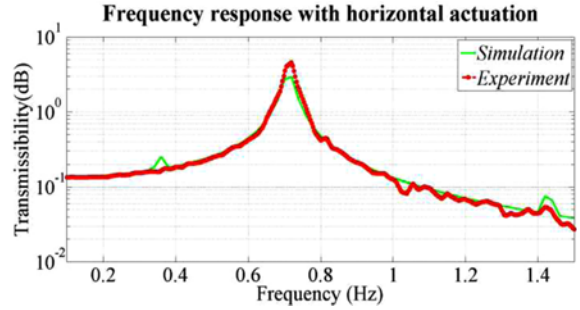

Fig. 6 Identification of open-loop frequency response function

the base is excited to have sinusoidal motions with frequencies of 0.1 to 1.5 Hz and vibrations of both the base and isolator top are measured using laser sensors. Then, the vibration transmissibility of Eq. (14) is obtained using a dynamic signal analyzer (HP 35670A).

$$\text{Transmissibility} = \frac{Y_m}{Y_B} \tag{14}$$

5. Simulation

5.1. Sensor model

Sensor dynamics is modeled with a low pass filter whose characteristic is shown as

$$G_s = \frac{\omega_c^2}{s^2 + \xi\omega_c s + \omega_c^2}. \tag{15}$$

where G_s is a transfer function of a sensor, ω_c is cut-off frequency and ξ is a damping ratio. Specifications of a displacement sensor, a velocity sensor and an accelerometer are shown in Table 3.

5.2 Voice coil motor (VCM) with current feedback loop

VCM is modeled considering current controller of the driver, mechanical characteristic and electrical parameters of VCM such as resistance and inductance of Table 2.[20]

5.3 Model validation

A simulation model for the active QZS isolator with horizontal actuation is built and verified by measuring open-loop frequency responses from VCM to the displacement of the isolator top, as shown in Fig. 6. Simulation using the model matches well with experimental measurement.

5.4 Simulations of control gain effects

The active isolation performances in relation with control gain variation are investigated by using both impulse disturbance rejection and vibration transmissibility.[20] Initially, gains are set as $a_1 = 0.01$, $a_2 = 3$, and $a_3 = 0.02$, and then each gain is increased by 10 times in sequence. The effects of displacement, velocity and nonlinear gains on impulse disturbance rejection are investigated, as shown in Fig. 7. Simulation results show that, although the velocity gain is very effective, the nonlinear gain has some effects on disturbance rejection. In addition, the effects of displacement, velocity and nonlinear gain

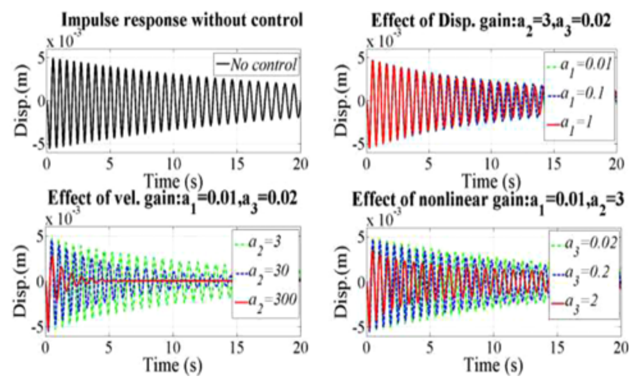

Fig. 7 Effect of control gains on impulse disturbance rejection

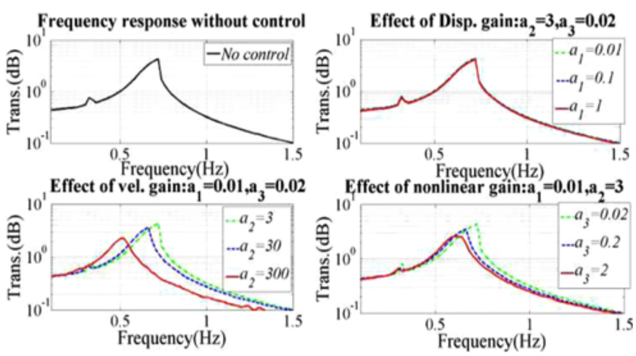

Fig. 8 Effect of control gains on vibration transmissibility

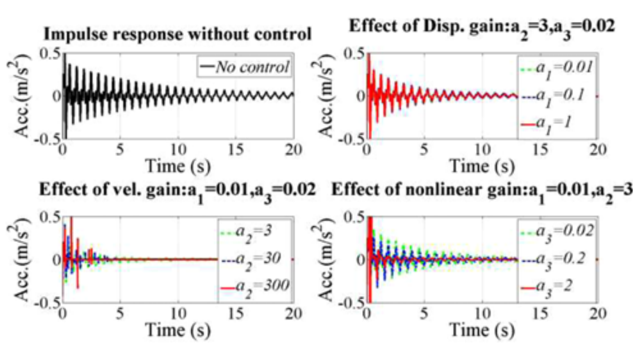

Fig. 9 Acceleration response according to various gains

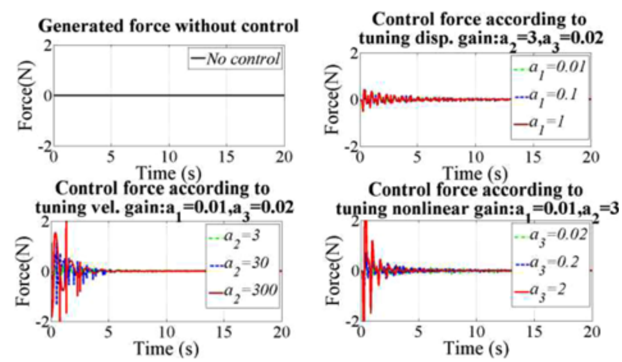

Fig. 10 Control force according to various gains

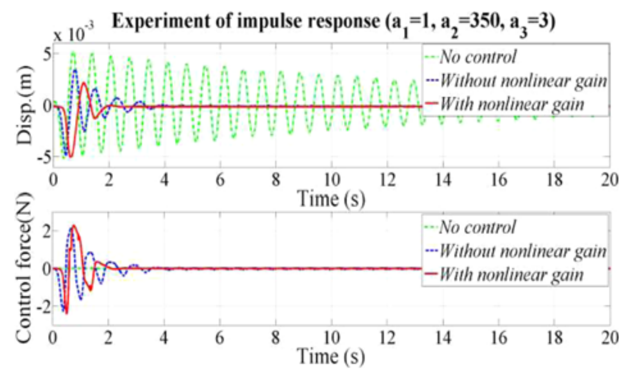

Fig. 11 Experiments for impulse disturbance rejection

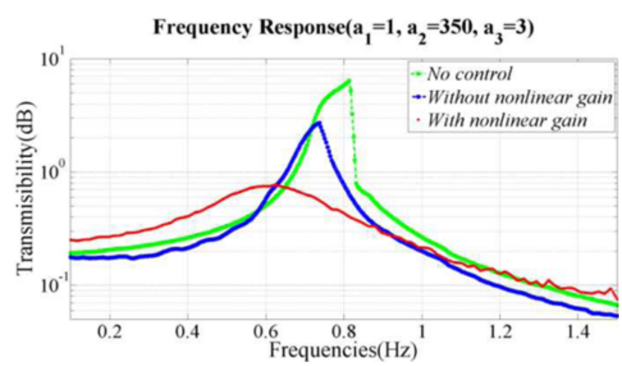

Fig. 12 Experiments for vibration transmissibility

variations on vibration transmissibility are shown in Fig. 8. The velocity gain reduces resonance peaks but increases transmissibility above resonance frequencies. The nonlinear gain can compensate for nonlinear dynamic characteristic of the isolator. Finally, the control gain is set as $a_1 = 1$, $a_2 = 350$, and $a_3 = 3$, considering the simulation results.

6. Experiments

6.1 Impulse response

For the passive QZS isolator with the natural frequency of 0.8 Hz, experiments of impulse disturbance rejection are performed with various control gains. Figure 9 and 10 show acceleration responses of payload and the control forces according to various control gains under impulse disturbance. Figure 11 shows displacement responses and corresponding actuator forces under impulse disturbance. The nonlinear control shows a better disturbance rejection performance than the linear control. The nonlinear control reduces the settling time by 50% more than the feedback control, although the maximum magnitudes of the control forces are similar.

6.2 Transmissibility

Vibration transmissibility of the isolator is experimentally measured as shown in Fig. 12. The linear feedback control reduces vibration resonance by 58 percent. However, it cannot remove the nonlinear characteristic of the system. The nonlinear control not only reduces the resonance magnitude by 91 percent, but can remove system nonlinearity of transmissibility jumping and lower the natural frequency to around 0.6 Hz.

7. Conclusion

A nonlinear control for an active quasi-zero stiffness isolator is investigated through both simulation and experiment. The nonlinear control algorithm is derived based on a Lyapunov function and isolator dynamic motion. The simulation model of the active QZS isolator is built to study the effects of control gains. To validate simulation results, the experiment is conducted and nonlinear control performance is examined. As shown in the experimental results of impulse disturbance and transmissibility, the settling time of system vibration response, the resonance magnitude and the natural frequency of system transmissibility are reduced significantly. In addition, the jumping nonlinearity of the system transmissibility is completely removed by the nonlinear control method. In summary, the active QZS isolator using the nonlinear control algorithm has good performance of vibration isolation and disturbance rejection as well.

ACKNOWLEDGEMENTS

This research was supported by the MKE (The Ministry of Knowledge Economy), Korea, under both the Convergence-ITRC(Convergence Information Technology Research Center) support program (NIPA-2012 C6150-1101-0004) supervised by the NIPA (National IT Industry Promotion Agency).

REFERENCES

1. Ibrahim, R. A., “Recent advances in nonlinear passive vibration isolators,” J. of Sound and Vibration, Vol. 314, No. 3-5, pp. 371-452, 2008.
2. Harris, C. M. and Piersol, A. G., “Shock and Vibration Handbook,” fifth ed., McGraw-Hill, 2002.
3. Rivin, E. I., “Passive Vibration Isolation,” ASME Press, 2001.
4. Platus, D. L., “Negative-stiffness-mechanism vibration isolation systems,” Proc. of SPIE, Vol. 1619, Vibration Control in Microelectronics, Optics and Metrology, pp. 44-54, 1991.
5. Minus K Technology, www.minusk.com
6. Zhang, J., Li, D., and Dong, S., “An ultra-low frequency parallel connection nonlinear isolator for precision instruments,” Key Engineering Materials, Vol. 257-258, pp. 231-236, 2004.
7. Schenka, M., Guestb, S. D., and Herdera, J. L., “Zero stiffness tensegrity structures,” Int. J. of Solids and Structures, Vol. 44, No. 20, pp. 6569-6583, 2007.
8. Tarnai, T., “Zero stiffness elastic structures,” Int. J. Mech. Sci., Vol. 45, No. 3, pp. 425-431, 2003.
9. Park, S. T. and Luu, T. T., “Techniques for optimizing parameters of negative stiffness,” Proc. IMechE part C: J. Mec. Eng. Sci., Vol. 221, No. 5, pp. 505-511, 2007.
10. Kovacic, I., Brennan, M. J., and Waters, T. P., “A study of a nonlinear vibration isolator with a quasi-zero stiffness characteristic,” J. of Sound and Vibration, Vol. 315, No. 3, pp. 700-711, 2008.
11. Ahn, H. J., “Performance limit of a passive vertical isolator,” J. of Mec. Science and Technology, Vol. 22, No. 12, pp. 2357-2364, 2008.
12. Carrella, A., Brennan, M. J., and Waters, T. P., “Static analysis of a passive vibration isolator with quasi-zero-stiffness characteristic,” J. of Sound and Vibration, Vol. 301, No. 3-5, pp. 678-689, 2007.
13. Trung, P. V., Kim, K. R., and Ahn, H. J., “Active Control of a Quasi-Zero Stiffness Isolator Using Flexures,” 12th International Symposium on Advanced Intelligent Systems, 2011.
14. Danh, L. T. and Ahn, K. K.., “Experimental investigation of a vibration isolation system using negative stiffness structure,” 11th IEEE Conference on Control, Automation and Systems, pp. 1582-1587, 2011.
15. Coppola, G. and Liu, K., “Control of a unique active vibration isolator with a phase compensation technique and automatic on/off switching,” J. of Sound and Vibration, Vol. 329, No. 25, pp. 5233-5248, 2010.
16. Kim, K. R., You, Y. H., and Ahn, H. J., “Optimal design of a QZS isolator using flexures for a wide range of payload,” Int. J. Precis. Eng. Manuf., Vol. 14, No. 6, pp. 911-917, 2013.
17. Ahn, H. J., “A Unified Model for Quasi-Zero-Stiffness Passive Vibration Isolators With Symmetric Nonlinearity,” Proc. of the ASME/IDETC, Paper No. DETC2010-28604, 2010.
18. Ahn, H. J. and Kim, K. R., “Active Control of Quazi-Zero Stiffness Isolators,” 4th Annual Dynamic Systems and Control Conference, 2011.
19. Carrella, A., Brennan, M. J., Waters, T. P., and Lopes, Jr. V., “Force and displacement transmissibility of a nonlinear isolator with high-static-low-dynamic-stiffness,” International Journal of Mechanical Sciences, Vol. 55, No. 1, pp. 22-29, 2012.
20. Kim, M. S. and Kim, J. H., “Design of a gain scheduled PID controller for the precision stage in lithography,” Int. J. Precis. Eng. Manuf., Vol. 12, No. 6, pp. 993-1000, 2011.